Published in final edited form as:
Gene Expr Patterns. 2013 December ; 13(8): . doi:10.1016/j.gep.2013.07.009.

The expression analysis of *Sfrs10* and *Celf4* during mouse retinal development

Devi Krishna Priya Karunakaran[1,#], **Sean Congdon**[1,#], **Thomas Guerrette**[1], **Abdul Rouf Banday**[1], **Christopher Lemoine**[1], **Nisarg Chhaya**[1], and **Rahul Kanadia**[1,*]

[1]Department of Physiology and Neurobiology, University of Connecticut, Storrs, Connecticut, 06269

Abstract

Processing of mRNAs including, alternative splicing (AS), mRNA transport and translation regulation are crucial to eukaryotic gene expression. For example, >90% of the gene in the human genome are known to undergo alternative splicing thereby expanding the proteome production capacity of a limited number of genes. Similarly, mRNA export and translation regulation plays a vital role in regulating protein production. Thus, it is important to understand how these RNA binding proteins including alternative splicing factors (ASFs) and mRNA transport and translation factors regulate these processes. Here we report the expression of an ASF, Serine-arginine rich splicing factor 10 (Sfrs10) and a mRNA translation regulation factor, CUGBP, elav like family member 4 (*Celf4*) in the developing mouse retina. Sfrs10 was expressed throughout postnatal (P) retinal development and was observed progressively in newly differentiating neurons. Immunofluorescence (IF) showed Sfrs10 in retinal ganglion cells (RGCs) at P0, followed by amacrine and bipolar cells, and at P8 it was enriched in red/green cone photoreceptor cells. By P22, Sfrs10 was observed in rod photoreceptors in a peri-nuclear pattern. Like Sfrs10, Celf4 was also observed in the developing retina, but with two distinct retinal isoforms. *In situ* hybridization (ISH) showed progressive expression of *Celf4* in differentiating neurons, which was confirmed by IF that showed a dynamic shift in Celf4 localization. Early in development Celf4 expression was restricted to the nuclei of newly differentiating RGCs and later (E16 onwards) it was observed in the initial segments of RGC axons. Later, during postnatal development, Celf4 was observed in amacrine and bipolar cells, but here it was predominantly cytoplasmic and enriched in the two synaptic layers. Specifically, at P14, Celf4 was observed in the synaptic boutons of rod bipolar cells marked by Pkc-α. Thus, Celf4 might be regulating AS early in development besides its known role of regulating mRNA localization/translation. In all, our data suggests an important role for AS and mRNA localization/translation in retinal neuron differentiation.

1. Introduction

The vertebrate retina is a part of the central nervous system and contains six neurons including, rod photoreceptors, cone photoreceptors, amacrine cells (AC), bipolar cells (BP), horizontal cells (HC), and retinal ganglion cells (RGCs) and one glial cell namely, Müller glia (MG). The retina has a stereotypic architecture with the nuclei of rod photoreceptors

[*]To whom correspondence should be addressed – rahul.kanadia@uconn.edu, 1-860-486-2692.
[#]Both authors contributed equally

and cone photoreceptors forming the outer nuclear layer (ONL), the nuclei of AC, BP, HC, and MG forming the inner nuclear layer (INL) and the nuclei of RGC forming the ganglion cell layer (GCL). In regards to AS in retinal development, very little is understood. The plethora of deep sequencing data has revealed the presence of single nucleotide polymorphisms (SNPs) across different populations and these SNPs could generate the complexity in the manner in which disease symptoms manifest. Specifically, SNPs can be detrimental if they occur in sequences responsible for regulating proper splicing. For example, 28% of all identified *Pax6* mutations are C-to-T affecting the CpG dinucleotides and 20% of these cause splicing error (Brown et al., 1998; Prosser and van Heyningen, 1998). Notably, the effect of SNPs on splicing and/or AS has not been investigated. Here the attempt is to shed light on the role of AS on retinal development and potentially disease by better understanding the role of ASFs during retinal development.

AS is the mechanism by which exons in protein coding genes are spliced in different combinations to generate vast proteome diversity. Indeed, >90% of the protein coding genes can produce multiple isoforms in a temporal and tissue specific manner (Pan et al., 2008; Wang et al., 2008). The process of AS is regulated by trans-acting factors called alternative splicing factors (ASFs). These factors either enhance or repress the recruitment of the spliceosome machinery to the pre-mRNA thereby facilitating the inclusion/exclusion of an exon in the final mRNA. SR proteins are a family of RNA binding proteins that act as exonic splicing enhancers (ESEs). Serine-Arginine rich splicing factor 10 (*Sfrs10*) belongs to this family of ASFs. Similarly, *Celf4* is a member of the *Celf* family, which are known ASFs, but Celf4 has been shown to regulate mostly translation regulation and the AS of very few genes (Barreau et al., 2006; Gallo and Spickett, 2010; Wagnon et al., 2012).

Sfrs10 is a mammalian homolog of drosophila Tra2beta, which regulates the AS of genes involved in sex determination of the fly (Baker, 1989; Hoshijima et al., 1991). In higher vertebrates, loss of *Sfrs10* results in mouse embryonic lethality around embryonic day (E) 7.5–8.5 (Mende et al., 2010). Brain specific knockout of Sfrs10 has shown to result in perinatal death in mice where pups die by P1 and show malformed brain (Grellscheid et al., 2011). The role of Sfrs10 in various tissues such as testis (Nayler et al., 1998; Grellscheid et al., 2011), intestinal (Fu et al., 2012) and vascular smooth muscle (Shukla and Fisher, 2008; Fu et al., 2012) has been studied. However, the role of Sfrs10 in retinal development remains unexplored.

In case of Celf4, a recent report showed that the constitutive loss of *Celf4* resulted in perinatal lethality and that heterozygous mice developed seizures, depending on the genetic background. This report suggests that the dosage of Celf4 protein is crucial to proper brain development and function (Wagnon et al., 2011). This idea is further bolstered by a recent report of a male patient with abnormal behavior, childhood seizures, myopia and obesity that was associated with the haploinsufficiency of Celf4 (Halgren et al., 2012). Moreover, loss of Celf4 in the brain results in seizures because the Celf4-null neurons have a lower action potential (AP) initiation threshold and a larger AP gain (Wagnon et al., 2012; Sun et al., 2013).

In this report, we show the spatial and temporal expression of Sfrs10 and Celf4 in retinal development. For both the genes, expression was observed in differentiating retinal neurons, which suggests that RNA processing might specifically play a role in terminal differentiation and/or synaptogenesis of retinal neurons. Moreover, Sfrs10 was enriched in newly differentiating red/green opsin cone photoreceptors, which can serve as a valuable early nuclear marker for cone photoreceptors. In case of Celf4, which has been shown to be predominantly cytoplasmic in adult brain neurons was found to be nuclear in early embryonic retinal neuron. This finding suggests that Celf4 might act as an ASF during early

retinal development and later in adult tissue it acts to regulate translation later in development. This transition in Celf4 function warrants further investigation.

2. Results

2.1 Sfrs10 is expressed across mouse retinal development

To determine whether *Sfrs10* was expressed during mouse retinal development, RT-PCR was performed across retinal development. The position of the primers used to amplify the coding sequence of *Sfrs10* is shown in Fig 1A. Expression was observed across retinal development with two distinct isoforms at postnatal day (P)4, P10 and P14 (Fig 1B). Sequence analysis of both these isoforms revealed that the isoform at 1234 bp was the canonical isoform encoding a full-length Sfrs10 protein. The higher MW isoform at 1511 bp was similar to the previously reported exon 2a containing isoform (Stoilov et al., 2004). Inclusion of exon 2a introduces a premature stop codon, which results in non-sense mediated decay of this transcript. *Gapdh* was used as a control (Fig 1B′). 5′ rapid amplification of cDNA ends (5′RACE) was performed to investigate whether alternate transcription start sites were being employed for Sfrs10 across retinal development. For this, PCR was employed on 5′-RACE ready cDNA library from retinae at different developmental time points. While the forward nested primers were in the 5′ linker sequence, the reverse primer was in exon 4 of Sfrs10. The PCR product was then purified and subjected to restriction digestion with EcoNI, which yielded two bands as predicted to be of 380 bp and 130 bp, respectively (Fig 1C). There was no change in the transcription start site across retinal development. Similar investigation across different developmental time points was carried out to check the alternate polyA signal usage in *Sfrs10* (NM_009186.4) as it contains three putative polyA signals (1672 bp, 1762 bp, 2247 bp). 3′ rapid amplification of cDNA ends (3′RACE) was employed with forward primers designed upstream of each polyA signal and a reverse primer in the linker sequence followed by restriction digestion with BsrI, which yielded two bands as predicted 407 bp and 230 bp. Again, the second PolyA signal at 1762 bp was utilized for Sfrs10 transcript across retinal development (Fig 1D).

2.2 Sfrs10 is expressed in differentiating retinal cells

Next, we employed IHC with AB#1 on mouse retinal section across postnatal development to ascertain the cell types expressing Sfrs10. At P0, Sfrs10 was observed in the nuclei in the ganglion cell layer (GCL) (Fig 2A). At P4, it was observed at the bottom of the outer neuroblastic layer (ONBL), besides the GCL (Fig 2B). Sporadic Sfrs10+ cells were also observed in the middle of the ONBL of the P4 retina. Next, Sfrs10 was costained with syntaxin which was localized to the cytoplasm of the Sfrs10+ nuclei. At P8, Sfrs10 was observed in all of the cell types in the INL including, Müller glia, horizontal cells, bipolar cells, and amacrine cells and the GCL (Fig 2D). In addition, in the newly formed ONL at P8, a few Sfrs10+ cells were observed. Similar pattern was observed in the ONL of P10 and P14 retinal sections (Fig 2E, F).

2.3 Sfrs10 marks red/green cone photoreceptors between P8-P14

The sporadic Sfrs10+ cells in the ONL at P8, P10 and P14 could either be rod photoreceptors or cone photoreceptors. To distinguish between these two possibilities, P8 and P10 retinal sections were stained for expression of Sfrs10 and red/green opsin. Three independent antibodies for Sfrs10 (AB#1, AB#2, and AB#3) were employed to confirm the specificity of the antibody (Fig 3A). Since the primary antibodies to detect both Sfrs10 and red/green opsin were raised in rabbit, they could not be detected simultaneously. Instead, serial IHC was performed, first with Sfrs10 followed by red/green opsin. Since Sfrs10 and red/green opsin are segregated into separate cellular compartments, i.e. nucleus and

cytoplasm, respectively, we were able to employ serial IHC. Here, it was observed that Sfrs10+ nuclei were enveloped by red/green opsin staining thereby confirming the identity of these cells to be red/green opsin cone photoreceptors (Fig 3B–D″). All three Sfrs10 antibodies showed similar pattern, thereby confirming the specific enrichment of Sfrs10 in red/green cone photoreceptors. Further, we performed immunoblot analysis on P0 retinal extracts with the two antibodies (AB#1 & AB#2), which again showed a single immunoreactive band at the expected molecular weight of Sfrs10 (Fig 3G, H).

2.4 Sfrs10 is peri-nuclear in rod photoreceptors

Analysis of Sfrs10 expression across postnatal development ending at P14 showed that the rod photoreceptors did not express Sfrs10. However, it is known that rod photoreceptors undergo rapid outer segment genesis between P13 and P17 and terminal differentiation including synapse formation is thought to be complete by P21 (Young, 1967; LaVail, 1973). To test whether Sfrs10 is expressed in rod photoreceptors during their terminal differentiation, IHC was performed for Sfrs10 on P22 retinal sections, which showed Sfrs10 expression in rod photoreceptors, albeit in a different pattern (Fig 4A). Unlike cone photoreceptors, where Sfrs10 was found in a diffused nuclear pattern, in rod photoreceptors it was localized in a peri-nuclear ring-like structure. Since photoreceptors do not have a large cytoplasmic space around the nucleus, it was not clear if Sfrs10 was in the cytoplasm or the nucleus. To further delineate the localization of Sfrs10, 6 μm retinal sections were costained with Sfrs10 and LaminB2 antibody, which marks the inner membrane of the nuclear envelope (Wakabayashi et al., 2011). Here Sfrs10 was found on the DAPI stained region, but did not overlap completely with LaminB2 thereby confirming its localization on the nuclear side of the nuclear envelope (Fig 4A–A″).

2.5 Two distinct isoforms of Celf4 are expressed in the developing mouse retina

RT-PCR analysis with primer pairs designed to interrogate the expression of the full-length (1.4 kb) coding sequence of Celf4 showed expression across retinal development at E12, E14, E16, E18, P0, P4, P8, P10 and P14 (Fig 5A). Next, PCR with a forward primer in exon-1 and a reverse primer that spanned exons 6 and 7 showed two distinct bands (Fig 5B). In contrast, PCR with a forward primer in exon-6 and reverse in exon-12 showed the expected single band (data not shown). All of these PCR products were cloned and sequenced followed by concatenation of the two products to generate two full-length retina-specific isoforms of Celf4. The isoform associated with the higher MW band observed with first PCR (exons 1-6/7) will be referred to as isoform A, while the other will be referred to as isoform B. Identification of the specific AS events in these two isoforms was done by curating all five isoforms of *Celf4* reported on the NCBI database and aligning their mRNA sequences to the retinal isoforms. This analysis showed three specific AS events occurring in the retina-specific isoforms of *Celf4*. The first AS event was the utilization of a cryptic splice donor in exon 3 that was spliced into a cryptic splice acceptor in exon 4. This event was observed in isoform A along with clone NM_001174074.1 and NM_001146293.1 (Fig 5C). The second AS event was the splicing of a cryptic splice donor in exon 5 to the canonical splice acceptor in exon 6. This AS event was observed in both and only in the retinal isoforms (Fig 5C). The third AS event was the splicing of the cryptic splice donor in exon 11 to the canonical splice acceptor in exon 12. This event was observed in both of the retinal isoforms along with clone NM_133195.3 and NM_001146293.1 (Fig 5C). The consequence of these AS events in the retinal isoforms is that they differ from each other by 11 AAs (GSSCLRQPPSQ), which are absent in isoform B (Fig 5D). Both these isoforms gain 6 AA (VSVTLG) by utilization of a cryptic splice donor in exon 5 and lose 20 AA (NVISSKVFVDRATNQSKCFG) by utilization of a cryptic splice donor in exon 11 (Fig 5C, D). In all, of the three AS events observed in the retinal isoforms two were found in the

other isoforms found in the NCBI database, but the addition of the 6 AA was unique to the retinal isoforms (Fig 6C, D).

2.6 Celf4 is expressed in newly differentiating neurons

Next, *In situ* hybridization (ISH) analysis was performed with an anti-sense DIG-labeled ribo-probe on retinal sections. *Celf4* RNA was detected in newly differentiating ganglion cells (GCs) at E16 (Fig 7A), which continues at E18 and P0 (Fig 7B, C). At P4, expression is also observed in newly differentiating amacrine cells (Fig 7D), followed by expression in newly differentiating bipolar cells at P8 (Fig 7E). This expression pattern was maintained at P14 (Fig 7F).

2.7 Celf4 localization is temporally regulated in the developing retina

Expression pattern of *Celf4* mRNA was subsequently confirmed by immunofluorescence for Celf4 on retinal sections across retinal development. Expression of Celf4 at E12 was lower and restricted to the differentiating retinal neurons (Fig 8A). Subsequently at E14, E16 and E18, expression of Celf4 was also observed in differentiating amacrine cells that are localized at the bottom of the ONBL abutting the newly forming inner plexiform layer (IPL) (Fig 8B, C, D). While Celf4 was detected in the nuclei of these differentiating neurons, it was also observed in the cytoplasm where it was enriched asymmetrically towards the newly forming projections. Specifically, Celf4 was enriched in the initial segment of the newly forming axons of the GCs (Fig 8F, inset). During postnatal development, at P0 and P4, Celf4 was observed in the outer plexiform layer (OPL) and IPL. Specifically, Celf4 was predominantly in the cytoplasm of bipolar and amacrine cells, but in the GCs, it was also detected in the nucleus (Fig 8G, H). At P14, the expression of Celf4 in bipolar cells and GCs was confirmed by Islet1+ nuclei encapsulated by Celf4+ immunofluorescence (Fig 9C). In contrast, Celf4 expression at P14 was not observed in Muller glia, which was shown by the lack of overlap of Celf4 and Glutamine Synthase staining (Fig 9F).

2.8 Celf4 overlaps with Pkc-α in rod bipolar cells

Interestingly, expression analysis of Celf4 with Pkc-α showed that Celf4 overlapped with Pkc-alpha at the synaptic boutons in the IPL and in the synapses in the newly forming OPL (Fig 10A). This colocalization suggested that Pkc-α might be the kinase phosphorylating Celf4. Interestingly, similar analysis performed in the adult retina (6 months) showed that Pkc-α immunofluorescence did not overlap with that of Celf4 in the synaptic boutons in the IPL (Fig 11E), but was maintained in the OPL (Fig 11D).

3. Discussion

ASFs are known to auto-regulate their levels. Indeed, Sfrs10 is one of the seven RNA-splicing associated genes that contain “exonic” class of “ultraconserved elements” (Ni et al., 2007). This class of RNA-binding proteins is shown to auto-regulate their levels by the inclusion of a stop codon containing exon, which is highly conserved in the vertebrate genome. This auto regulation is thought to be critical for the maintenance of cellular homeostasis of various classes of RNA-binding proteins. This is concordant with the expression pattern of Sfrs10 observed across the retinal development. The higher MW isoform contains exon 2a, which introduces premature stop codon, rendering the transcript to NMD pathway and regulating the levels of the lower MW canonical isoform. Sfrs10 expression in postnatal retinal development follows the order of terminal differentiation of retinal neurons. Ganglion cells are the first cells to differentiate, followed by amacrine and horizontal cells at P4. The costaining of syntaxin and Sfrs10 in the ONBL of P4 retina suggests that they are mostly likely differentiating amacrine and horizontal cells. This observation is in agreement with the previous report where it was shown that syntaxin marks

both differentiating amacrine and horizontal cells in the postnatal developing retina (Alexiades and Cepko, 1997). At P8, bipolar cells, amacrine cells, and cone photoreceptors differentiate followed by rod photoreceptors by P21. This suggests that Sfrs10-mediated AS is involved in genes that regulate the terminal differentiation of the retinal cells. Further, Sfrs10 expression specifically in red/green cone photoreceptors suggests that Sfrs10-mediated AS is specifically required by this subset of cone photoreceptors during development and for their maintenance. This observation would make Sfrs10 one of the first alternative splicing factors to mark red/green cone photoreceptors at P8. Additionally, it would be a valuable nuclear marker of cone photoreceptors at this stage in retinal development as well as in retinal diseases.

Celf4 is a member of the CUG binding proteins (CUGBP) that are implicated in the pathogenesis of the disease myotonic dystrophy (Leroy et al., 2006). The expression in differentiating neurons suggests that Celf4 might regulate genes specifically involved in terminal differentiation. Indeed, loss of Celf4 in the brain results in seizures caused by aberrant electrophysiological properties of the Celf4-null neurons (Sun et al., 2013). Specifically, they show that loss of Celf4 results in increased Na(v)1.6 protein levels, which was coincident with aberrant localization of Ankyrin G in the initial segment. This phenotype revealed the possible role of Celf4 in regulating mRNA transport/localization/translation of a subset of genes, which are involved in terminal differentiation. A similar role can be envisaged for Celf4 in the retina, where it shows a shift into the cytoplasm across development and is also observed in the initial segment of newly differentiating RGCs (Fig 8F). At P14, Celf4 was colocalized with Pkc-α, which marks rod bipolar cells. Specifically, the overlap was observed in the synaptic boutons, where phosphorylation of Celf4 might mediate synaptic function. In the adult retinal sections the overlap of Celf4 with Pkc-α shifts from being in both the IPL and the OPL to just in the OPL. This shift may indicate yet another transition in the role of Celf4 during terminal differentiation to maintenance and retinal function. Finally, in the adult retina, Celf4 was observed in the outer segments of cone photoreceptors, which could be cross-reactivity to an unrelated protein. However, the antibody employed here was the same as the one used in a previous report where it was employed in the Celf4-null brain sections and did not show any cross-reactivity. However, it is still possible that in the retina it is cross-reacting to a protein that is not expressed in the brain. Regardless, the Celf4 antibody can serve to mark adult cone photoreceptor outer segments. Another possibility is that Celf4 is indeed expressed in cone photoreceptor outer segments and it serves a novel function that warrants future investigations.

3.1 Conclusion

Here we show that ASFs including Sfrs10 and Celf4 were expressed in differentiating retinal neurons and are maintained in the adult retina. Their expression implies the usage of RNA processing including AS and mRNA translation by retinal neurons during terminal differentiation and function. The extent to which AS is employed during neuronal differentiation and function is not well understood and our data on the expression of Sfrs10 suggests that it might play a crucial role. Specifically, mRNA processing including AS by Sfrs10 and AS, transport/translation by Celf4 might play a vital role in regulating complex signal transduction during neuronal differentiation and function.

4. Materials and methods

4.1 Animal Procedures

All procedures with mice were performed in accordance with the animal protocol approved by Institutional Animal Care and Use Committee at the University of Connecticut. The CD1 or the ICR mice from Charles River Laboratory, MA, were employed for all experiments.

4.2 Reverse transcriptase-polymerase chain reaction (RT-PCR)

Retinae from different developmental time points in CD1 mice (E12, E14, E16, E18, P0, P4, P10, and P14) were harvested and total RNA prepared in Trizol following the manufacturer's protocol (Invitrogen). For cDNA synthesis, 1μg of total RNA from retinae harvested at various time points was used (Kanadia et al., 2006). PCR to detect *Sfrs10* isoforms was performed with a forward (5′-AGCTTGACAGCTTCAGGAAAGGCC- 3′) and a reverse (5′-ATCCCAGCTCTATGGCAGGTTTCAG- 3′) primer for 30 cycles (95°C for 30 seconds; 58°C for 30 seconds; 72°C for 1.5 minutes). Gapdh was used as the control. PCR used to detect *Gapdh* was performed with a forward (5′ – ACAGTCAAGGCCGAGAATGGGAA –3′) and a reverse (5′ – TCAGATGCCTGCTTCACCACCTTCT – 3′) primer and same temperature profile as described above. All PCR products were resolved on a 2.5% agarose gel. PCR to detect the coding sequence of *Celf4* was performed with a forward (5′-ATGTATATAAAGATGGCCACGTTAGCAAAC-3′) and a reverse (5′-TCAGTACGGGCGATTGGCGTCTTT-3′) primer for 30 cycles (95°C for 30 seconds; 58°C for 30 seconds; 72°C for 2 minutes). PCR to detect *Celf4* isoforms was performed with a forward primer in exon 1 (5′-ATGTATATAAAGATGGCCACGTTAGCAAAC-3′) and a reverse primer at the junction between exon 6 and 7 (5′-TGCTGCATCAGTGCCTGAGCATA-3′) for 30 cycles (95°C for 30 seconds; 58°C for 30 seconds; 72°C for 30 seconds). The aforementioned protocol was used for PCR to detect the c-terminus of *Celf4* by employing a forward primer at exon 6/7 (5′-TATGCTCAGGCACTGATGCAGCA-3′) and a reverse primer in exon 12 (5′-TCAGTACGGGCGATTGGCGTCTTT-3′). PCR to generate the probe for *in situ* hybridization was performed with a forward (5′-GAACGCTTCCAGATAGGCATGAAG-3′) and reverse primer (5′-AAATAGAGATGCTCAGTGGCGGCCT-3′) for cycles (95°C for 30 seconds; 58°C for 30 seconds; 72°C for 2 minutes). All PCR products were resolved on a 2.0% agarose gel.

4.3 Section *in situ* hybridization

In situ hybridization was performed on 16 μm cryosections of CD1 murine retina as previously described (Trimarchi et al., 2007). PCR amplified product (refer to 4.2) of *Celf4* 3′ UTR was used to generate the probe.

4.4 5′ RLM-RACE

Retinae from different developmental time points in CD1 mice (E15.5, E17.5, P0, P5, and P14) were harvested and total RNA was prepared as described above. 5′ RNA ligase-mediated rapid amplification of cDNA ends (5′ RLM-RACE) (First Choice RLM-RACE kit from Invitrogen) was employed to determine the transcription initiation site(s) of *Sfrs10* mRNA. This method amplifies cDNA only from full-length, capped mRNA, therefore allowing identification of the actual 5′ ends of mRNAs. Total RNA from different time points were first treated with Calf Intestine Alkaline Phosphatase (CIP) to remove the 5′ phosphate from degraded mRNA, rRNA, and tRNA. Samples were then treated with Tobacco Acid Pyrophosphatase (TAP) to remove the cap structure of intact mRNAs, leaving a 5′ phosphate group on this mRNA subset only, followed by ligation of an RNA adapter to the decapped mRNAs. Reverse transcription and subsequent PCR amplification using adapter-specific outer and inner primers (provided in the kit) and gene-specific reverse primer were performed to allow the 5′ ends of mRNA transcripts to be mapped. The gene specific reverse primer of *Sfrs10* is 5′-CCAAACACGCCAAGACAACAGTTG-3′. Instead of cloning, the PCR products were purified and then subjected to restriction digestion with EcoNI to check if the same product is obtained throughout development. Uncut and cut products were resolved on 2% agarose gels.

4.5 3′RACE

Retinae from different developmental time points in CD1 mice (E15.5, E17.5, P0, P5, and P14) were harvested and total RNA was prepared as described above. Reverse transcription was performed using Moloney Murine Leukemia Virus Reverse Transcriptase (M-MLV RT) with the addition of 3′RACE adapter to the RNA mix. cDNAs obtained were used for PCR amplification with gene-specific forward primer and adapter-specific outer and inner primers. The sequence of gene-specific primer is 5′-CTTTCTAAATATCAATGCTTAACCAGAACCATTC-3′. Next, the PCR products were purified and then subjected to restriction digestion with BsrI to check if the same product is obtained throughout development. Uncut and cut products were resolved on 2% agarose gels.

4.6 Immunofluorescence

All of the experiments were performed on 10–16 μm cryosections obtained from different time points in CD1 mice except for the 6 month retina which was obtained from C57/BL6 mice. The cryosections were first hydrated in phosphate-buffered saline (PBS, pH 7.4) and washed three times (5 minutes each at room temperature (RT)), followed by incubation with PBTS buffer (1X PBS with 0.1% triton-X 100, 0.2% BSA and 0.02% SDS) for an hour at RT. Primary antibody (AB#1-rabbit anti-Sfrs10, 1:750, Fitzgerald inc., Product #70R-1420; AB#2-rabbit anti-Sfrs10, 1:500, Sigma-Aldrich, Product # AV40528; AB#3 – rabbit anti-Sfrs10, 1:500, Cemines, Product # AB/SF100; mouse anti-syntaxin-1 (HPC-1), 1:300, Santacruz biotechnologies Inc., Product # sc12736; Celf4/Brunol4 antibody, 1:300, Santacruz biotechnologies Inc., Product # sc84712; mouse anti-islet1, 1:300, Developmental Studies Hybridoma Bank, Product# 40.2D6; mouse anti-Pkc-α, 1:300, Calbiochem, Product # OP74; mouse anti-glutamine synthase, 1:300, Chemicon International, Product # MAB302) was incubated in PBTS buffer overnight at 4°C. Sections were washed with PBTS buffer containing 4′, 6-diamidino-2phenylindole (DAPI) (Roche diagnostics) 10 times (15 minutes each at RT). Following the washes, secondary antibody (anti-rabbit antibody conjugated with Alexa488, 1:750, Product # 21206, anti-mouse conjugated with Alexa 568, 1:750, Product # A10037, Invitrogen) was incubated in PBTS buffer overnight at 4°C. Sections were washed with PBTS buffer 7 times (15 minutes each at RT), rinsed with PBS and covered with Prolong gold anti-fade reagent (Invitrogen) and coverslip glass.

4.7 Serial IF

Here the aforementioned IF protocol was employed with one modification. Upon completion of the nuclear antigen detection by the first antibody, (primary – rabbit anti-Sfrs10, 1:750 and secondary – Alexa488, 1:750), a 10′/RT incubation with 4% paraformaldehyde was conducted. Subsequently, the cytoplasmic antigen detection by the second antibody (primary – rabbit anti - red/green opsin, 1:300, Millipore, Product # AB5405 and secondary – Alexa568, Invitrogen, 1:750, Product # 11011) was performed.

4.8 Image Acquisition and 3D reconstruction

Confocal fluorescence microscopy was performed using Leica SP2. Images were subsequently processed using IMARIS (Bitplane Inc., CA) and Adobe Photoshop CS4 (Adobe Systems Inc., CA).

Acknowledgments

This work was supported by grants from National Institute of Neurological Disorder and Stroke (P30-P30NS069266) and National Eye Institute (R00- R00EY019547) to RK.

References

Alexiades MR, Cepko CL. Subsets of retinal progenitors display temporally regulated and distinct biases in the fates of their progeny. Development. 1997; 124(6):1119–31. [PubMed: 9102299]

Baker BS. Sex in flies: the splice of life. Nature. 1989; 340(6234):521–4. [PubMed: 2505080]

Barreau C, Paillard L, Mereau A, Osborne HB. Mammalian CELF/Bruno-like RNA-binding proteins: molecular characteristics and biological functions. Biochimie. 2006; 88(5):515–25. [PubMed: 16480813]

Brown A, McKie M, van Heyningen V, Prosser J. The Human PAX6 Mutation Database. Nucleic Acids Res. 1998; 26(1):259–64. [PubMed: 9399848]

Fu K, Mende Y, Bhetwal BP, Baker S, Perrino BA, Wirth B, Fisher SA. Tra2beta protein is required for tissue-specific splicing of a smooth muscle myosin phosphatase targeting subunit alternative exon. J Biol Chem. 2012; 287(20):16575–85. [PubMed: 22437831]

Gallo JM, Spickett C. The role of CELF proteins in neurological disorders. RNA Biol. 2010; 7(4):474–9. [PubMed: 20622515]

Grellscheid S, Dalgliesh C, Storbeck M, Best A, Liu Y, Jakubik M, Mende Y, Ehrmann I, Curk T, Rossbach K, et al. Identification of evolutionarily conserved exons as regulated targets for the splicing activator tra2beta in development. PLoS Genet. 2011; 7(12):e1002390. [PubMed: 22194695]

Halgren C, Bache I, Bak M, Myatt MW, Anderson CM, Brondum-Nielsen K, Tommerup N. Haploinsufficiency of CELF4 at 18q12.2 is associated with developmental and behavioral disorders, seizures, eye manifestations, and obesity. Eur J Hum Genet. 2012; 20(12):1315–9. [PubMed: 22617346]

Hoshijima K, Inoue K, Higuchi I, Sakamoto H, Shimura Y. Control of doublesex alternative splicing by transformer and transformer-2 in Drosophila. Science. 1991; 252(5007):833–6. [PubMed: 1902987]

Kanadia RN, Shin J, Yuan Y, Beattie SG, Wheeler TM, Thornton CA, Swanson MS. Reversal of RNA missplicing and myotonia after muscleblind overexpression in a mouse poly(CUG) model for myotonic dystrophy. Proc Natl Acad Sci U S A. 2006; 103(31):11748–53. [PubMed: 16864772]

LaVail MM. Kinetics of rod outer segment renewal in the developing mouse retina. J Cell Biol. 1973; 58(3):650–61. [PubMed: 4747920]

Leroy O, Dhaenens CM, Schraen-Maschke S, Belarbi K, Delacourte A, Andreadis A, Sablonniere B, Buee L, Sergeant N, Caillet-Boudin ML. ETR-3 represses Tau exons 2/3 inclusion, a splicing event abnormally enhanced in myotonic dystrophy type I. J Neurosci Res. 2006; 84(4):852–9. [PubMed: 16862542]

Mende Y, Jakubik M, Riessland M, Schoenen F, Rossbach K, Kleinridders A, Kohler C, Buch T, Wirth B. Deficiency of the splicing factor Sfrs10 results in early embryonic lethality in mice and has no impact on full-length SMN/Smn splicing. Hum Mol Genet. 2010; 19(11):2154–67. [PubMed: 20190275]

Nayler O, Cap C, Stamm S. Human transformer-2-beta gene (SFRS10): complete nucleotide sequence, chromosomal localization, and generation of a tissue-specific isoform. Genomics. 1998; 53(2): 191–202. [PubMed: 9790768]

Ni JZ, Grate L, Donohue JP, Preston C, Nobida N, O'Brien G, Shiue L, Clark TA, Blume JE, Ares M Jr. Ultraconserved elements are associated with homeostatic control of splicing regulators by alternative splicing and nonsense-mediated decay. Genes Dev. 2007; 21(6):708–18. [PubMed: 17369403]

Pan Q, Shai O, Lee LJ, Frey BJ, Blencowe BJ. Deep surveying of alternative splicing complexity in the human transcriptome by high-throughput sequencing. Nat Genet. 2008; 40(12):1413–5. [PubMed: 18978789]

Prosser J, van Heyningen V. PAX6 mutations reviewed. Hum Mutat. 1998; 11(2):93–108. [PubMed: 9482572]

Shukla S, Fisher SA. Tra2beta as a novel mediator of vascular smooth muscle diversification. Circ Res. 2008; 103(5):485–92. [PubMed: 18669920]

Stoilov P, Daoud R, Nayler O, Stamm S. Human tra2-beta1 autoregulates its protein concentration by influencing alternative splicing of its pre-mRNA. Hum Mol Genet. 2004; 13(5):509–24. [PubMed: 14709600]

Sun W, Wagnon JL, Mahaffey CL, Briese M, Ule J, Frankel WN. Aberrant sodium channel activity in the complex seizure disorder of Celf4 mutant mice. J Physiol. 2013; 591(Pt 1):241–55. [PubMed: 23090952]

Trimarchi JM, Stadler MB, Roska B, Billings N, Sun B, Bartch B, Cepko CL. Molecular heterogeneity of developing retinal ganglion and amacrine cells revealed through single cell gene expression profiling. J Comp Neurol. 2007; 502(6):1047–65. [PubMed: 17444492]

Wagnon JL, Briese M, Sun W, Mahaffey CL, Curk T, Rot G, Ule J, Frankel WN. CELF4 regulates translation and local abundance of a vast set of mRNAs, including genes associated with regulation of synaptic function. PLoS Genet. 2012; 8(11):e1003067. [PubMed: 23209433]

Wagnon JL, Mahaffey CL, Sun W, Yang Y, Chao HT, Frankel WN. Etiology of a genetically complex seizure disorder in Celf4 mutant mice. Genes Brain Behav. 2011; 10(7):765–77. [PubMed: 21745337]

Wakabayashi T, Mori T, Hirahara Y, Koike T, Kubota Y, Takamori Y, Yamada H. Nuclear lamins are differentially expressed in retinal neurons of the adult rat retina. Histochem Cell Biol. 2011; 136(4):427–36. [PubMed: 21842415]

Wang ET, Sandberg R, Luo S, Khrebtukova I, Zhang L, Mayr C, Kingsmore SF, Schroth GP, Burge CB. Alternative isoform regulation in human tissue transcriptomes. Nature. 2008; 456(7221):470–6. [PubMed: 18978772]

Young RW. The renewal of photoreceptor cell outer segments. J Cell Biol. 1967; 33(1):61–72. [PubMed: 6033942]

Highlights

- Sfrs10 and Celf4 are expressed in differentiating neurons in the postnatal retina
- Sfrs10 marks red/green cone photoreceptors
- Sfrs10 is perinuclear in rod photoreceptors
- Celf4 has two distinct retinal isoforms which differ by 11 amino acids
- Celf4 shifts from the nucleus to the cytoplasm across retinal development

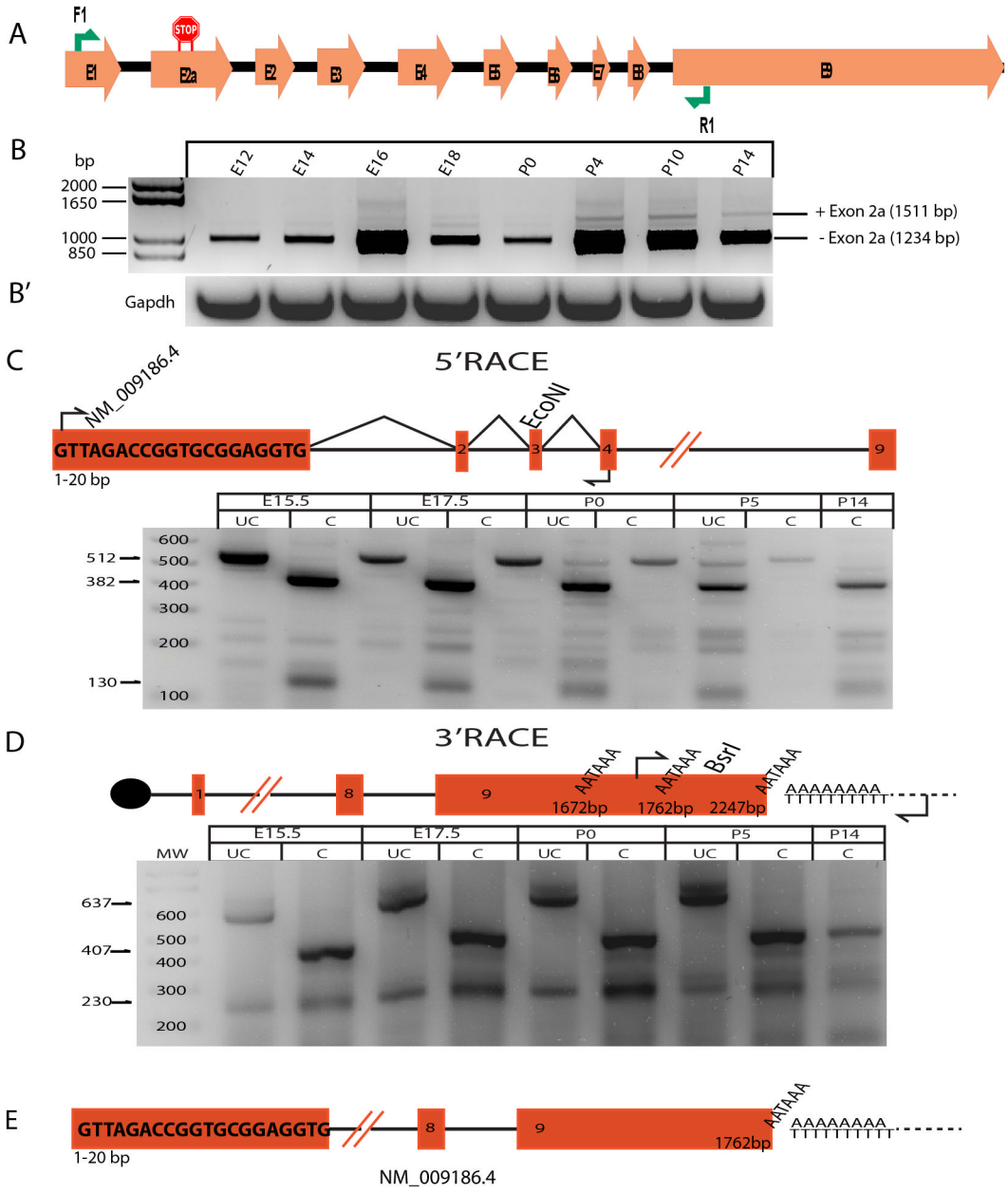

Fig 1. Expression analysis of *Sfrs10* during mouse retinal development

A: Schematic representation of Sfrs10 gene showing exons (orange arrows, E1–E9), intron (black line) and the primers (green arrows, F1 &R1) used for RT-PCR analysis. **B:** Gel image showing two RT-PCR products of Sfrs10, top band (+ exon 2a), bottom band (exon 2a). **B′:** Gel image showing *Gapdh* expression. **C:** 5′RACE analysis across retinal development. Shown here is the position of the primers and the restriction site for EcoNI. **D:** 3′RACE analysis across retinal development. Shown here is the position of the primers and the restriction site for BsrI. **E:** Schematic representation of the gene after the RACE analysis.

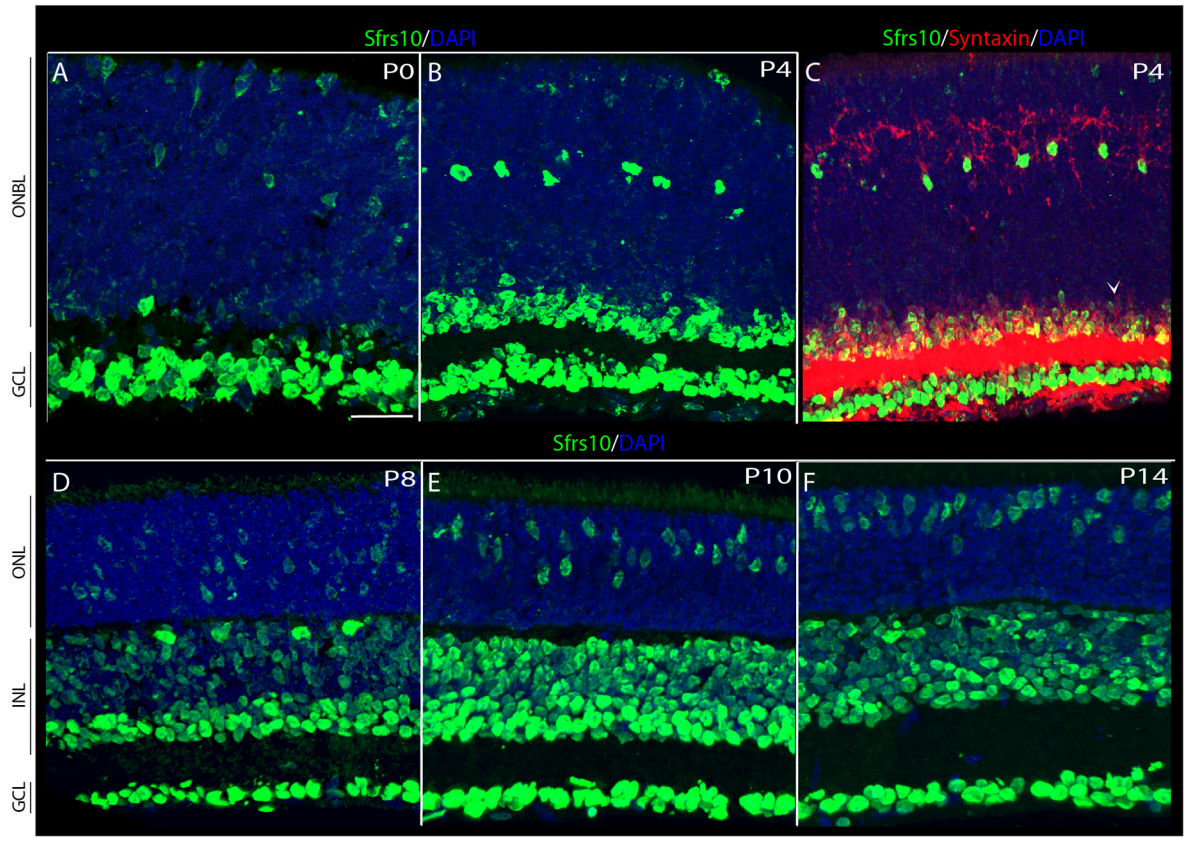

Fig 2. SFRS10 expression across postnatal retinal development

A, B, D, E, F: Immunohistochemistry across postnatal retinal development with rabbit anti-Sfrs10 (green). Nuclei are marked with DAPI (blue). Scale bar: 30μm. GCL, Ganglion cell layer; INL, Inner Nuclear layer; ONL, Outer nuclear layer; ONBL, Outer neuroblastic layer. **C:** Immunohistochemistry for Sfrs10 (green) co-stained for Syntaxin (red) which marks differentiating amacrine cells. Nuclei are marked with DAPI (blue).

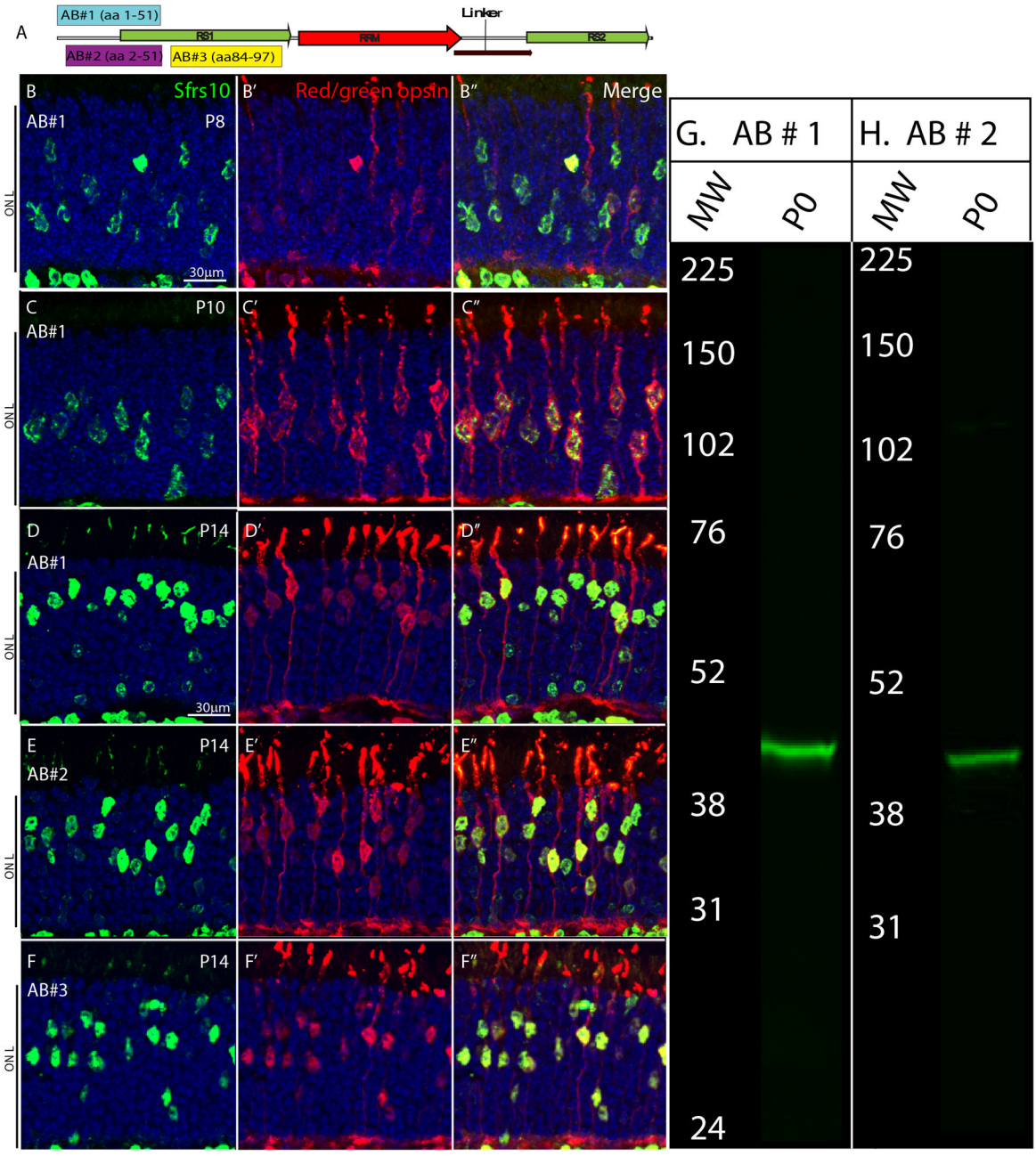

Fig 3. Specific enrichment of SFRS10 in red/green cone photoreceptors

A: Schematic of Sfrs10 protein with RRM (RNA recognition motif) flanked by two RS (Serine-Arginine dipeptide rich) domains. Above and below the schematic are boxes representing the epitope positions for antibody (AB) #1 (blue box, amino acids 1-51), AB#2 (purple box, amino acids 2-51) and AB#3 (yellow box, amino acids 84-97). **B–D″:** Serial IHC with rabbit anti-Sfrs10 AB#1 (green) and rabbit anti-red/green opsin (red) and the merged image at P8 (B-B″), P10 (C-C″) and P14 (D-D″). **E- E″:** Serial IHC with rabbit anti-Sfrs10, AB#2 (green) and rabbit anti-red/green opsin (red) and the merged image (E″). **F - F″:** Serial Immunohistochemistry with rabbit anti-Sfrs10, AB#3 (green) and rabbit anti-red/green opsin (red) and the merged image (F″). Scale bars 30 µm. **G, H:** Immunoblot analysis for Sfrs10 (AB#1 (G), AB#2 (H)) on retinal protein extracts from P0 mouse.

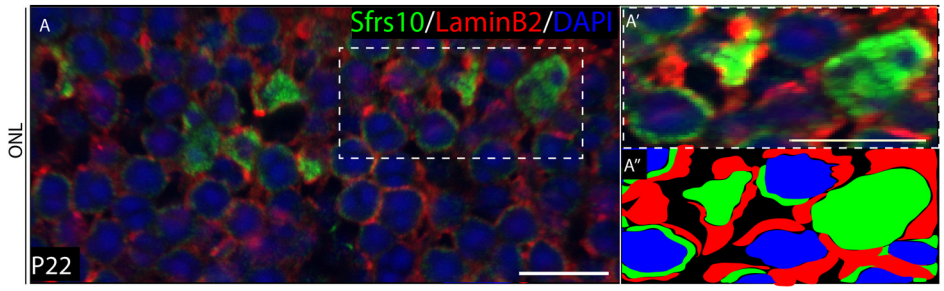

Fig 4. Differential expression of SFRS10 in rod photoreceptors versus cone photoreceptors

A: IHC on P22 retinal section for SFRS10 (green), laminB2 (red). Nuclei are marked with DAPI (blue). Shown here is the outer nuclear layer. Scale bar 5μm **A′:** Magnified image of the boxed region in (B) showing perinuclear localization of SFRS10 in laminB2 positive cells. Scale bar 3 μm. **A″:** Schematic representation of SFRS10 localization observed in A.

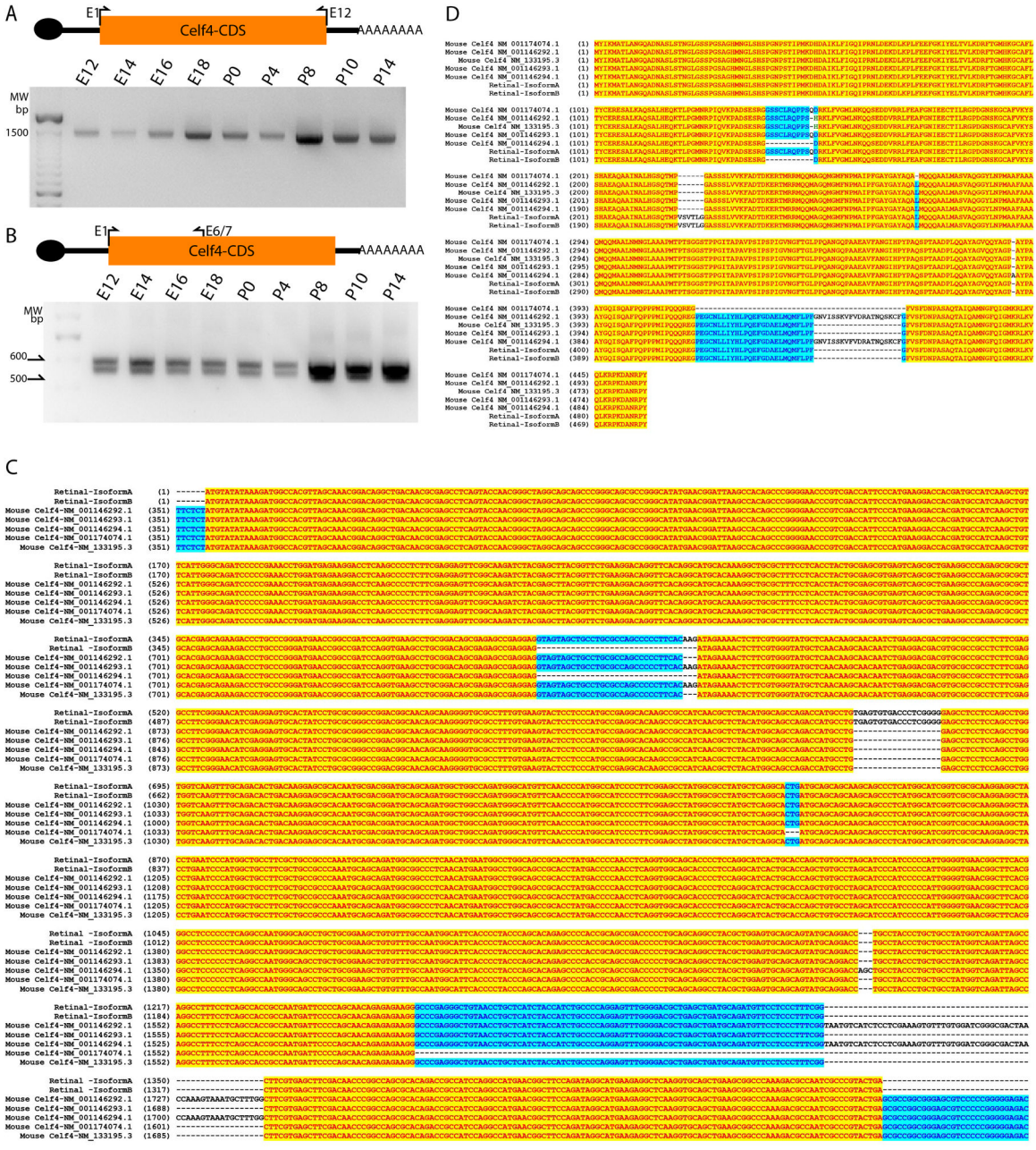

Fig 5. Expression analysis of *Celf4* during mouse retinal development

A: Schematic representation of Celf4 mRNA with the position of the forward (exon 1) and reverse primers (exon 12) is shown above the image of the gel-image showing full coding sequence of *Celf4* throughout retinal development. **B:** Schematic representation of *Celf4* mRNA with the position of the forward (exon 1) and reverse primers (exon 6/7) is shown above the gel-image showing the isoforms of *Celf4* across retinal development **C:** Multiple sequence alignment of nucleotides of the concatenated retinal isoforms of *Celf4* and those from the NCBI database. **D:** Multiple sequence alignment of the corresponding AA of retinal Celf4 isoforms and those from NCBI.

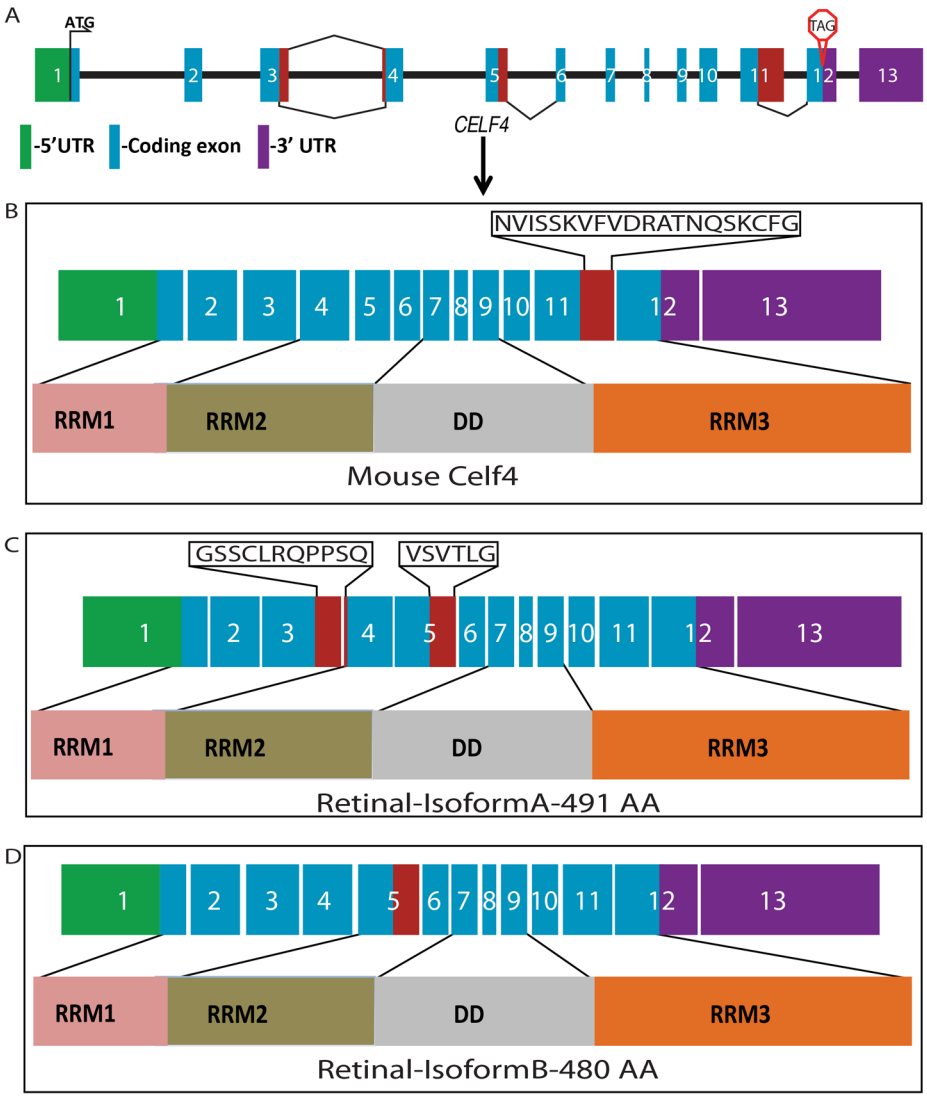

Fig 6. Schematic representation of *Celf4* isoforms and Celf4 protein domains in the retina

A: Schematic representation of the *Celf4* gene with color codes indicating the 5′-UTR (green), AA coding (blue), and the 3′UTR (purple). The start and stop codons are also indicated and the cryptic splicing utilized in the retinal isoforms are shown as red boxes and their splicing is shown by the connecting lines. **B:** Schematic representation of *Celf4* mRNA with its exons and the corresponding proteins domains of Celf4. The sequence shown in the box is the sequence that would be included if the entire exon were included in the mRNA. **C:** Schematic representation of Celf4 isoform A with its corresponding protein product**. D:** Schematic representation of Celf4 isoform B with its corresponding protein product.

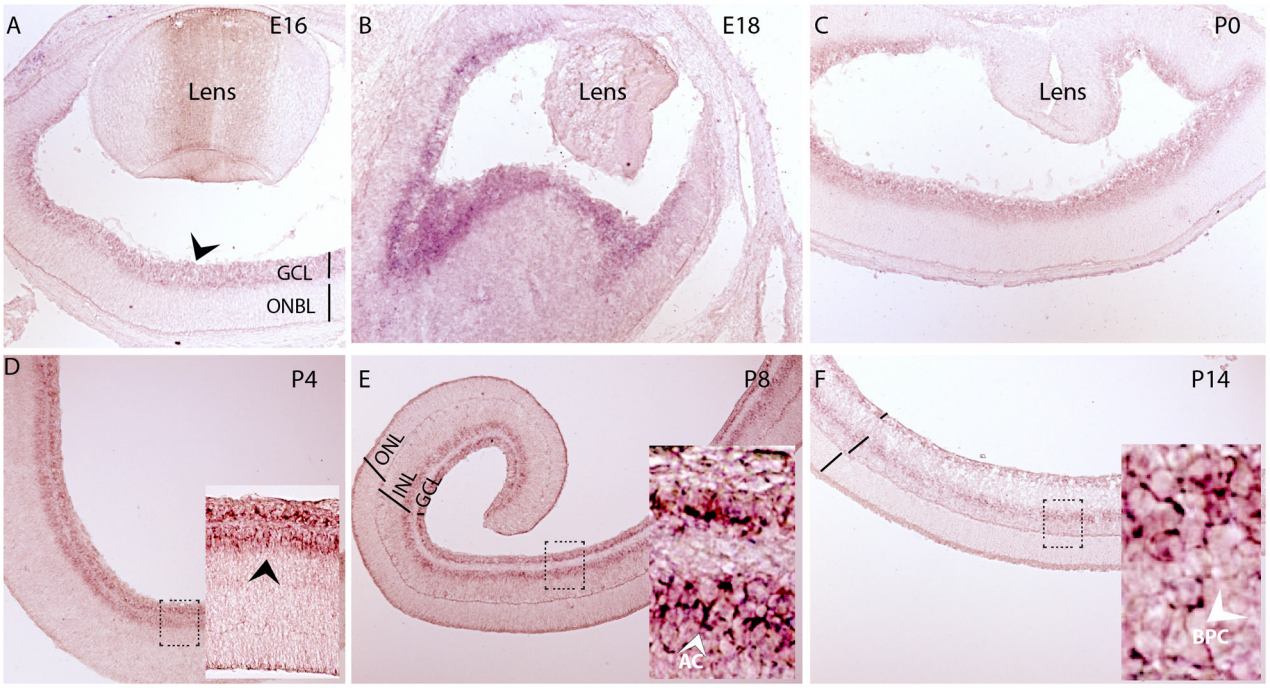

Fig 7. Expression analysis of *Celf4* mRNA by *In situ* hybridization across mouse retinal development

A-F: *In situ* hybridization for *Celf4* mRNA across the retinal development. Inset in **D, E** and **F** show magnified images of the GCL and INL. Black arrows in **A, D** and **F** indicate the regions that express *Celf4* mRNA.

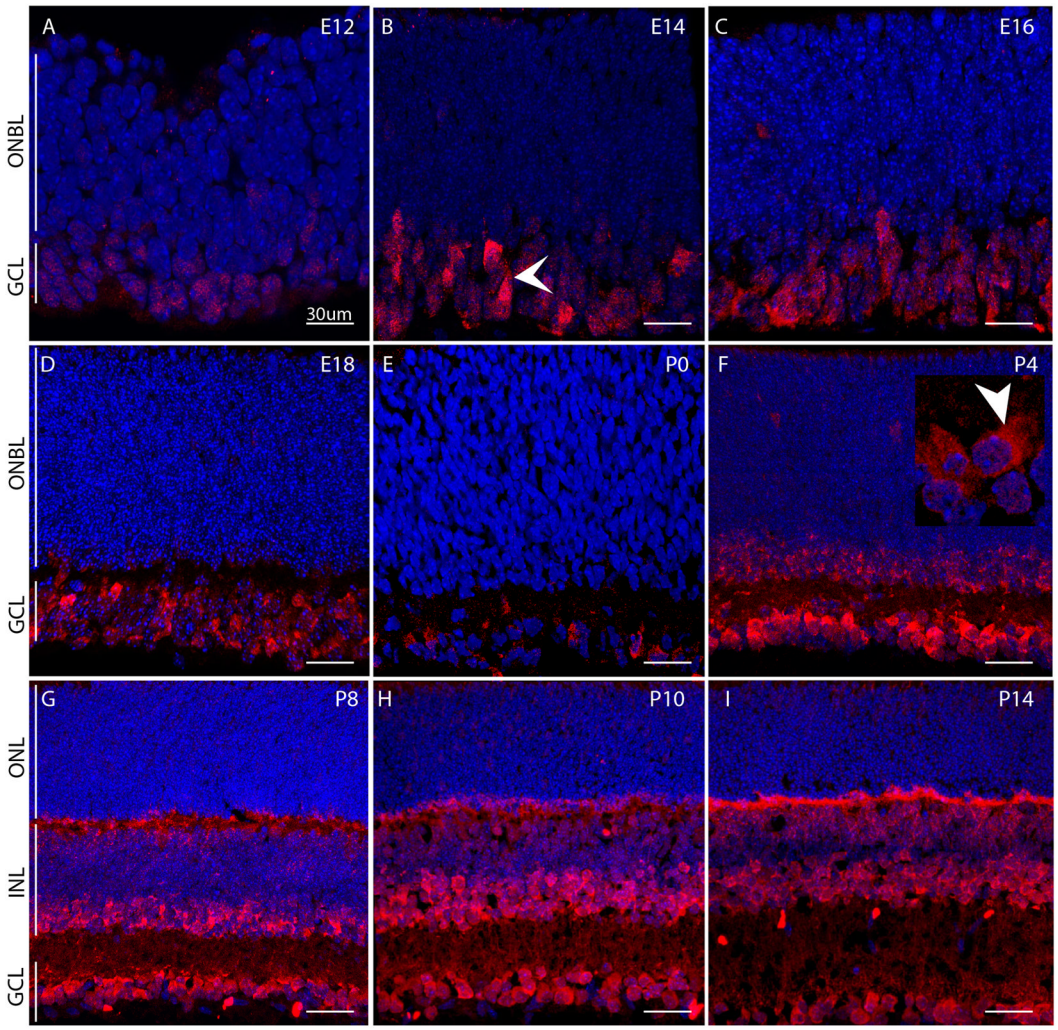

Fig 8. Celf4 expression across mouse retinal development

A–I: IHC on retinal section across developmental timepoints, E12, E14, E16, E18, P0, P4, P8, P10 and P14 with rabbit anti-Celf4 (red); DAPI marks the nuclei and the scale bar is 30μm. Inset in F shows magnified image of the GCL, which shows the cytoplasmic localization of Celf4, which is indicated by solid white arrows in B and F. GCL, Ganglion cell layer; INL, Inner Nuclear layer; ONL, Outer nuclear layer; ONBL, Outer neuroblastic layer.

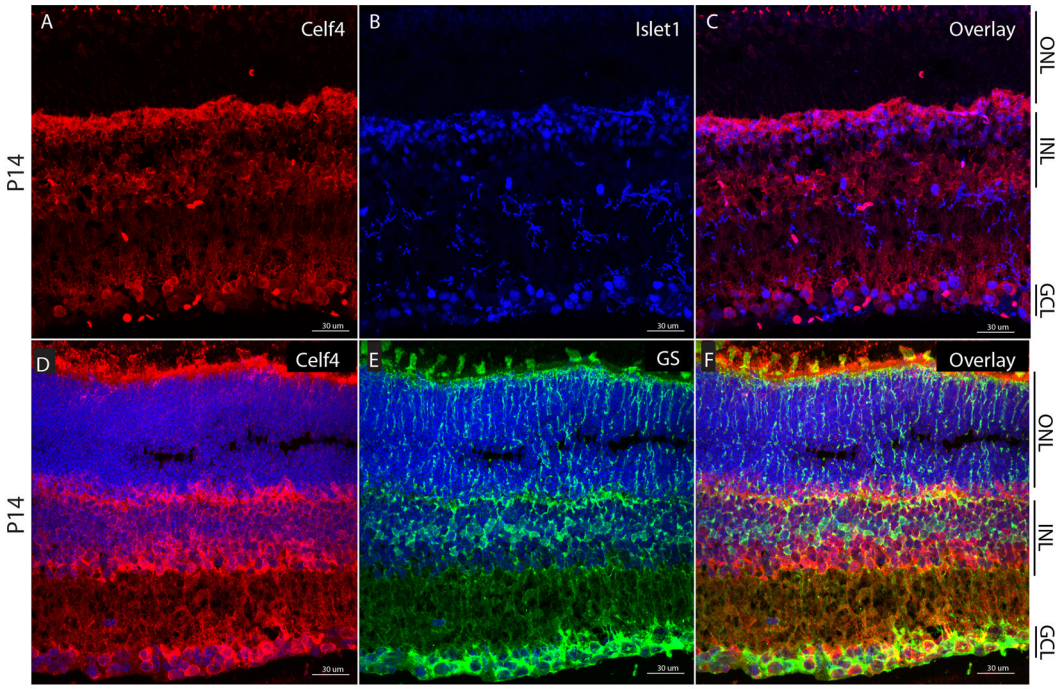

Fig 9. Lack of Celf4 expression in Muller glia

A: IHC of P14 retina with Rabbit anti-Celf4 (red), **B:** Mouse anti-Islet1 (blue), **C:** Overlay of Celf4 and Islet1. **D:** Overlay of Rabbit anti-Celf4 (red) and DAPI (blue), **E:** Overlay of Mouse anti-Glutamate Synthase (green) and DAPI (blue), **F:** Overlay of Celf4, Glutamine Synthase and DAPI.

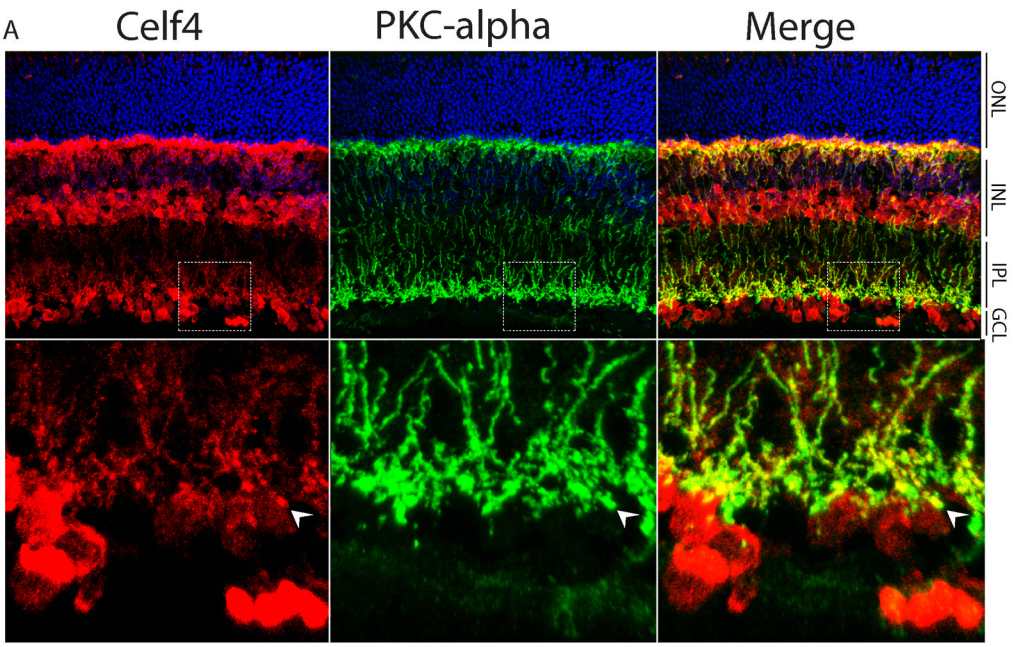

Fig 10. Celf4 overlaps with Pkc-α in retinal bipolar synaptic boutons

A: IHC on P14 retinal sections for Celf4 (red), Pkc-α (green) and overlap of the two signals is shown under merge. Magnified image of the white box drawn in the top panel is shown below.

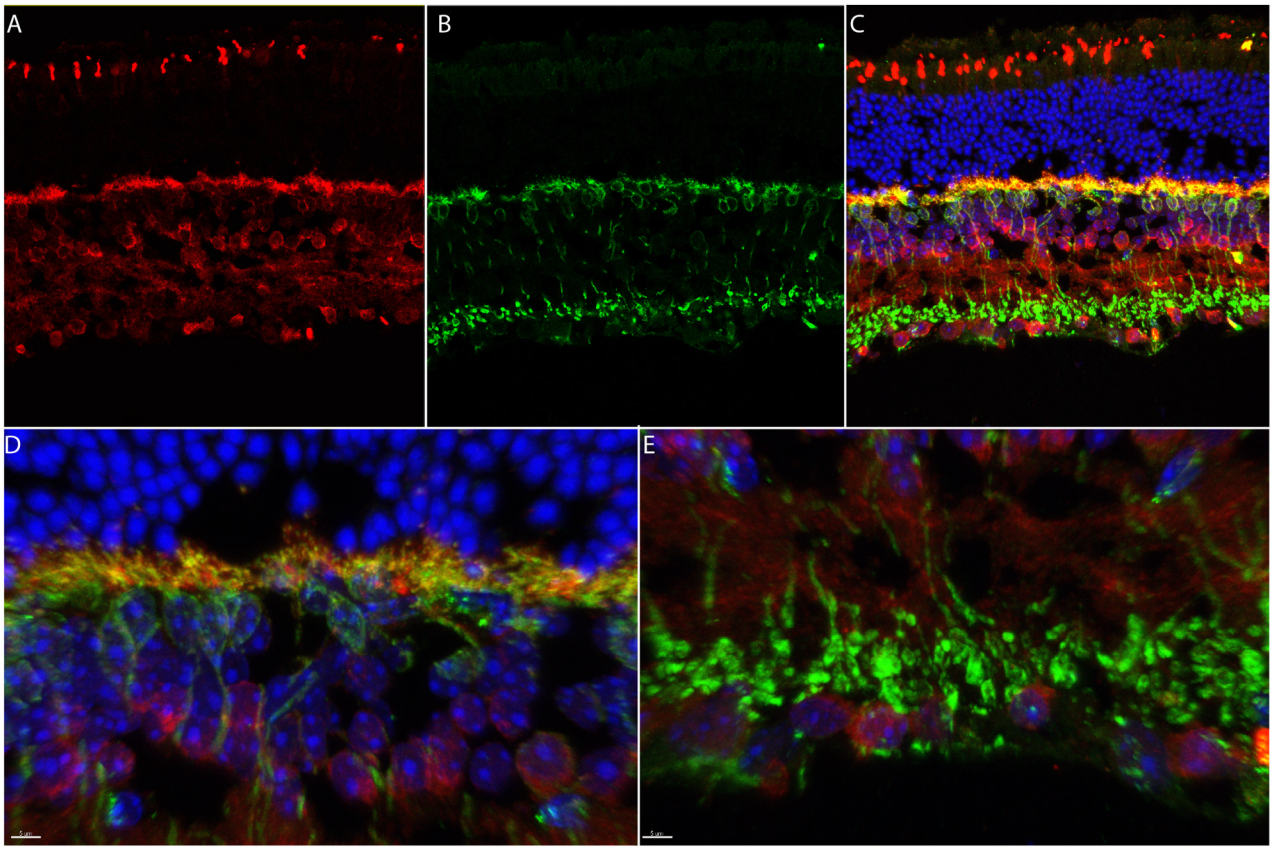

Fig 11. Shift in overlapping pattern of Celf4 and Pkc-α in the adult retina

A: IHC of 6-month-old C57/Bl6 mouse retina with rabbit anti-Celf4 (red), **B:** Mouse anti-Pkc-α (green), **C:** Overlay between Celf4 and Pkc-α. DAPI marks all the nuclei (blue). **D:** High magnification of the outer plexiform layer with Celf4 shown in red and Pkc-α shown in green. **E:** High magnification of the inner plexiform layer with Celf4 (red) and Pkc-α (green).